

PAPER View Article Online
View Journal | View Issue



Cite this: Nanoscale, 2019, 11, 6192

Triple conjugated carbon dots as a nano-drug delivery model for glioblastoma brain tumors†

Sajini D. Hettiarachchi, ^{Da} Regina M. Graham, ^{Db} Keenan J. Mintz, ^{Da} Yiqun Zhou, ^{Da} Steven Vanni, ^b Zhilli Peng^a and Roger M. Leblanc ^D *

Most of the dual nano drug delivery systems fail to enter malignant brain tumors due to a lack of proper targeting systems and the size increase of the nanoparticles after drug conjugation. Therefore, a triple conjugated system was developed with carbon dots (C-dots), which have an average particle size of 1.5–1.7 nm. C-dots were conjugated with transferrin (the targeted ligand) and two anti-cancer drugs, epirubicin and temozolomide, to build the triple conjugated system in which the average particle size was increased only up to 3.5 nm. *In vitro* studies were performed with glioblastoma brain tumor cell lines SJGBM2, CHLA266, CHLA200 (pediatric) and U87 (adult). The efficacy of the triple conjugated system (dual drug conjugation along with transferrin) was compared to those of dual conjugated systems (single drug conjugation along with transferrin), non-transferrin C-dots-drugs, and free drug combinations. Transferrin conjugated samples displayed the lowest cell viability even at a lower concentration. Among the transferrin conjugated samples, the triple conjugated system (C-dots-trans-temo-epi (C-DT)) was more strongly cytotoxic to brain tumor cell lines than dual conjugated systems (C-dots-trans-temo (C-TT) and C-dots-trans-epi (C-ET)). C-DT increased the cytotoxicity to 86% in SJGBM2 at 0.01 µM while C-ET and C-TT reduced it only to 33 and 8%, respectively. Not only did triple conjugated C-DT increase the cytotoxicity, but also the two-drug combination in C-DT displayed a synergistic effect.

Received 6th November 2018, Accepted 17th February 2019 DOI: 10.1039/c8nr08970a

rsc.li/nanoscale

1. Introduction

Cancer is one of the leading causes of death by disease world-wide. Although less common than some cancers, malignant brain tumors remain a significant cause of morbidity and mortality in adults and children. In fact, brain tumors are the number one cause of pediatric cancer deaths. One of the most common types of brain tumors are gliomas and the prognosis for high-grade gliomas such as glioblastoma (GBM) remains dismal. Obstacles to successful treatment include: the inability to surgically remove the entire tumor, the lack of effective drugs able to cross the blood-brain barrier (BBB) at therapeutic levels, and the development of multidrug resistance (MDR), which contributes to tumor recurrence and patient relapse. The development of MDR is multifactorial and includes the increased drug efflux by ATP-dependent

Florida 33146, USA. E-mail: rml@miami.edu; Fax: +1-305-284-6367;

pumps, intracellular detoxification, and increased DNA repair anti-apoptosis mechanisms.

Nanoparticles, including carbon dots (C-dots), have been used in drug delivery systems to improve drug solubility, increase drug half-life and improve drug accumulation at the cancerous site. The Enhanced Permeability and Retention (EPR) effect promotes the accumulation of nanoparticles in the tumor tissues with the help of leaky blood vessels and abnormal lymphatic drainage. Therefore, localization of nanoparticle drug delivery systems on tumors reduces drug side effects, enhances the drug bio-availability and improves drug tolerance. 10-12

However, EPR only enables the accumulation of nanoparticles in the tumor tissues. The poor cellular uptake of the drug delivery system still limits the anticancer drug dosage, which limits the therapeutic ultimately Furthermore, the physiological structures comprising the BBB, which is composed of an endothelial cell monolayer surrounded by pericytes and astrocytes, 14-16 significantly decrease the amount of the nanoparticles able to cross the BBB and enter the tumor. To overcome this problem, nanoparticles should conjugate with BBB-targeting and tumor-targeting ligands to improve the efficacy of the brain tumor drug delivery systems. Therefore, this nanotechnology is a promising route for cellular imaging and drug delivery. 17,18

^aDepartment of Chemistry, University of Miami, 1301 Memorial Drive, Coral Gables,

Tel: +1-305-284-2194

^bDepartment of Neurological Surgery, Miller School of Medicine, University of Miami, Miami, Florida 33136, USA. E-mail: rgraham@med.miami.edu; Tel: +1-305-321-4972

[†]Electronic supplementary information (ESI) available. See DOI: 10.1039/c8nr08970a

The single nano drug delivery system is the most popular drug delivery system. The problem with a single anticancer drug is that, with the long-term delivery, the likelihood of drug resistance increases, which ultimately lowers its therapeutic efficacy. Therefore, to improve the treatment response, dual drug delivery systems are currently being investigated. The major advantages of the combinational drug therapy are: the synergistic effect, overcoming the MDR, and the reduction of toxicity. In single drug delivery systems, the drug exerts the anticancer activity only through a specific pathway, but dual drug systems can act in multiple pathways to increase the anticancer activity. Therefore, the overall therapeutic efficacy was found to be greater in combinational drug therapy than the sum of the effects of each individual drug. The combinational therapy therefore exerts a synergistic effect on anticancer activity at a lower dose of drugs.¹⁹ Conversely, combinational therapy can even be inhibitory if one drug suppresses the anticancer activity of the other drug. Therefore, combinational therapies will not be synergistic for all the drug combinations.

The second advantage of dual drug systems is related to the development of multidrug resistance (MDR). Brain tumors demonstrate intra-tumor heterogeneity, which refers to the phenomenon that the cells within the tumor are not identical and can differ in gene expression and response to therapy. Therefore, although a single drug may effectively kill a subpopulation of tumor cells, the resistant population will continue to grow. Combinatorial therapy reduces the chances of development of drug resistance by targeting more than one cell population and increasing the potential for tumor cell death and tumor demise.

Also finally, most of the chemotherapeutic agents are pumped out of the cell by drug efflux pumps. In a dual drug combination, one of the drugs can be utilized to block these efflux pumps as an advantage. In contrast, if none of the drugs used in the combinational therapy inhibits the efflux pumps, it is challenging to deliver the drugs inside the cell. Therefore, a proper targeting system is still required to deliver the chemotherapeutics into the cell.

Several studies have been performed to achieve dual drug delivery systems using different types of nanoparticles for cancer treatments. Still these studies have limitations which hinder their application in brain tumor treatments. Shen et al.20 studied a dual drug system composed of an anthracycline drug, doxorubicin, and an efflux pump inhibitor, verapamil, by using magnetic nanoparticles, which showed a high drug efficacy, but the overall particle size increased up to 144 nm. Song et al. 21 have reported the delivery of fluorescein and rhodamine B with a mesoporous silica nanoparticle electrospun composite mat, but again the particle size after the drug loading is around 163 nm, which is still too large to cross the BBB. ^{20,21} Aryal *et al.* ²² have reported dual drug pre-covalent conjugation of paclitaxel and gemcitabine through hydrolysable ester bonds, which poses a risk of releasing the drugs before they reach the cancerous site. Furthermore, the lipid coated polymeric nanoparticles they used were 80 nm in size.²² So even though these studies used dual moiety drug delivery systems, most of them are devoid of a proper targeting system, as well as bigger in size. For brain tumor treatment, smaller nanoparticle size is preferred since it has been demonstrated that smaller nanoparticles can more easily cross the blood-brain barrier and more rapidly penetrate the tumor tissue.^{23,24} Therefore, an optimal brain tumor drug delivery system should be tumor cell targeted, deliver more than one chemotherapeutic drug, and be smaller in size. In this study, we synthesized a triple conjugated targeted drug delivery system with a dual drug and non-toxic C-dots as the nanocarrier. The carboxylic acid functionalized C-dots have been covalently conjugated via the amide linkages with the targeting ligand transferrin, and the anti-cancer agents epirubicin and temozolomide (Fig. 1).

C-dots are photoluminescent nanomaterials which are 1-10 nm in size. ²⁵⁻²⁸ They are prominent in many applications due to their unique characteristics. C-dots show high photoluminescence, wavelength dependent/independent emission, water dispersity, high cell membrane permeability, excellent biocompatibility and non-toxicity, which make them superior candidates for the drug delivery process and biomedical applications. 28-33 On the surface of the C-dots mainly exist C, H and O elements.²⁶ In general, for broad application, the surface of C-dots is functionalized with either carboxylic acids or amine groups, which is beneficial to the covalent conjugation with drugs and other targeted molecules through the amide linkages.26,34

Folic acid and transferrin are widely used bio-ligands. Transferrin is a blood plasma glycol protein which contains 679 amino acids with a high molecular mass (MW 80 kDa). Li et al.30 have identified that C-dots-transferrin can cross the blood-brain barrier and enter the central nervous system (CNS) by using zebrafish as the biological model.³⁰ Recently, transferrin has also been identified as a good cancer targeting ligand due to the overexpression of the transferrin receptors at the surfaces of many types of cancer cells.35 In the current study, transferrin was used only as a targeted ligand which increased the cell penetration.

One of the most widely used anti-cancer drugs for nanodelivery is doxorubicin, which is of the anthracycline family. Epirubicin (epi) is a 4'-epimer of doxorubicin and, compared to doxorubicin, is less cardio-toxic and better tolerated. Like other anthracyclines, epi intercalates into DNA inducing DNA cleavage assisted by topoisomerase II and inhibits the synthesis of DNA and RNA. In addition to the formation of reactive oxygen species, which increase oxidative damage, 14,36 epirubicin is also approved for the treatment of breast cancer and is being studied as a treatment for solid malignant tumors of the stomach, lungs, ovaries and lymphomas.

Temozolomide is a DNA alkylating/methylating agent which causes the DNA strand breakage and apoptosis of cells. This is a second generation orally administered imidazotetrazine derivative, which has been shown to increase the overall survival of GBM patients from 12.1 to 14.6 months.³⁷ However, during the activation process, temozolomide readily hydrolyses in the physiological pH into active 5-(3-methyltriazen-1-yl) and

Paper Nanoscale

Fig. 1 Schematic illustration of a triple conjugated system composed of transferrin, epirubicin and temozolomide on the carboxylic acid functionalized C-dots. The drawings are not according to the exact scale and the ratio. Only a 1:1:1:1 ratio of -COOH: transferrin: epirubicin: temozolomide is shown for the sake of clarity.

imidazole-4-carboxamide (MTIC) and finally into aminoimidazole-4-carboxamide (AIC) (Fig. S1†). Even though temozolomide can easily cross the BBB by itself, MTIC or AIC cannot do so.³⁸ Therefore, temozolomide conjugation on C-dots (prior to the hydrolyzation) is more important to increase the therapeutic efficacy.

Herein, this triple conjugated C-dot model is used to deliver the chemotherapeutic drugs epirubicin and temozolomide into glioblastoma brain tumor cells with the help of transferrin that enters the cell via receptor mediated endocytosis.

2. **Materials**

Carbon nano powder, N-hydroxysuccinimide (NHS), 1-ethyl-3-(3-dimethylaminopropyl) carbodiimide (EDC), epirubicine hydrochloride and temozolomide were bought from Sigma Aldrich (St Louis, MO). Iron saturated human transferrin (HOLO) was obtained from MP Biomedicals (Solon, OH). Sulfuric acid (98%) and nitric acid (68-70%) were purchased from ARISTAR (distributed by VWR, Radnor, PA). Thermo Fisher Scientific (Waltham, MA, USA) provided the dialysis tubing with a molecular weight cutoff (MWCO) of 3500 Da and a Sephacryl S-300 column was obtained from GE Healthcare (Uppsala, Sweden) for size exclusion chromatography (SEC). Deionized (DI) water was obtained from a Modulab 2020 water purification system (San Antonio, TX) and it has a resistivity of 18 M Ω ·cm and a surface tension of 72.6 mN m⁻¹ at 20.0 \pm

0.5 °C. Pediatric brain tumor cell lines SJGBM2, CHLA200 (glioblastoma) and CHLA266 (atypical teratoid/rhabdoid tumor) were procured from Children's Oncology Group (COG, Lubbock, TX) while the adult glioblastoma cell line U87 was obtained from American Type Culture Collection (ATCC, Manassas, VA, USA). The cell lines were cultured in RPMI-1640 (Thermo Fisher Scientific, Waltham, MA, USA) supplemented with 10% heat-inactivated fetal bovine serum and 1% penicillin-streptomycin; both of them were purchased from Gemini Biosciences (West Sacramento, CA). All cell lines were routinely tested for mycoplasma using a LookOut mycoplasma PCR detection kit from Sigma Aldrich (St Louis, MO) according to the manufacturer's instructions and maintained at 37 °C in a humidified 5% CO2 incubator.

3. Methods

Synthesis of black C-dot powder

Carboxylic acid functionalized black C-dot powder was synthesized following Li et al.29 via the acidic oxidation of carbon nano powder. 1 g of carbon nano powder was mixed with 36 mL sulfuric acid and 12 mL nitric acid. The mixture was refluxed for 15 h at 110 °C in an oil bath. After it cooled down, unreacted acids were neutralized in an ice bath using saturated sodium hydroxide solution (pH 14). Then the mixture was vacuum filtered to remove unreacted carbon powder. The supernatant was kept in an ice bath to precipitate unwanted salts. A piece of sodium sulfate was added to avoid super-saturNanoscale Paper

ation. The above step was repeated one more time to remove salts further. The excess water was evaporated out from the supernatant and then the mixture was followed by washing with chloroform (60 mL) three times. Then the solution was centrifuged at 3000 rpm for 30 min. Next, the solution was transferred to a dialysis bag (MWCO 3500 Da) and dialyzed with 4 L of DI water for 5 days. DI water was changed every 4–10 h. After that, the solution was again heated at around 75–85 °C to concentrate it and then it was placed in a rotovap to evaporate off water to obtain the C-dots.

3.2. Synthesis of the C-dots-transferrin-epirubicintemozolomide complex (triple system; C-DT)

8 mg of C-dots were dissolved in 3 mL of 25 mmol L⁻¹ phosphate buffer solution (PBS) (pH 7.4). Then 17.78 mg 1-(3-dimethylaminopropyl)-3-ethylcarbodiimide hydrochloride (EDC) dissolved in 0.5 mL of PBS was added in to the C-dot solution. The mixture was stirred at room temperature for 20 min. Then 10.7 mg of N-hydroxysuccinimide (NHS) dissolved in 0.5 mL of PBS was added to the mixture. After 20 min of stirring, 1 mL transferrin (3 mg mL⁻¹) solution was added. After another 45 min, 4.0 mg of epirubicin and 13.5 mg of temozolomide were added, each of which had been dissolved in 0.5 mL of dimethyl sulfoxide (DMSO). The entire mixture was stirred at room temperature overnight. Then the mixture was dialyzed with the 3500 MWCO dialysis bag for 4 days. The DI water was replaced every 4-10 h. Then the pre-dialyzed sample was further purified by SEC. The resultant eluent was collected in different test tubes and analyzed by UV-vis and fluorescence spectroscopy to identify the samples containing C-dotsepirubicin-temozolomide-transferrin (C-DT). The identified samples were frozen at -80 °C and lyophilized for 4 days to obtain the powdered product.

3.3. Synthesis of the C-dots-epirubicin–transferrin complex (dual system; C-ET)

The same procedure as above was followed by starting the synthesis with 8 mg of C-dots. Then EDC and NHS addition was performed with the same amounts as described in section 3.2 within the same interval of time. Then the same amount of transferrin was added followed by the addition of 4.0 mg of epirubicin after the same interval of time. The purifications were conducted as above, and the powdered product was taken out after lyophilization.

3.4. Synthesis of the C-dots-temozolomide-transferrin complex (dual system; C-TT)

The exact same procedure as above was followed but adding 13.5 mg of temozolomide only, instead of 4.0 mg of epirubicin.

3.5. Synthesis of C-dots-epirubicin–temozolomide, C-dots-epirubicin and C-dots-temozolomide complexes (non-transferrin complexes)

8.0 mg of C-dots were activated by adding EDC and NHS in the same amount as those described in section 3.2. Then 13.5 mg

of temozolomide and 4.0 mg of epirubicin were added into two different reaction vessels separately to synthesize C-dots-temozolomide and C-dots-epirubicin. Finally, 13.5 mg of temozolomide and 4.0 mg of epirubicin were both added together with 8.0 mg of C-dots to synthesize the C-dots-epirubicin-temozolomide conjugate.

3.6. Characterization

The synthesized conjugates (20 $\mu g \text{ mL}^{-1}$) were tested by UV-vis spectroscopy in a 1 cm quartz cell using a Shimadzu UV-2600 spectrometer. Then the fluorescence emission spectra of the same samples were recorded using a Horiba Jobin Yvon Fluorolog-3 with a slit width of 5 nm for both excitation and emission. The solid FTIR study was performed using a PerkinElmer FTIR (Frontier) spectrometer using the attenuated total reflection (ATR) technique, which uses the ATR prism alone as the background. Matrix-assisted laser desorption ionization time of flight (MALDI-TOF) was performed using a Bruker autoflex speed spectrometer. Transmission electron microscopy (TEM) studies were conducted with a JEOL 1200× TEM and atomic force microscopy (AFM) studies were conducted using an Agilent 5420 atomic force microscope in the tapping mode. Each characterization study was repeated with different batches of C-dot conjugates to verify the consistency of the data and the stability of the complexes.

3.7. In vitro studies

The effect of chemotherapy or conjugation to C-dots with and without transferrin was evaluated in the pediatric brain tumor cell lines SJGBM2, CHLA266, and CHLA 200 and the adult brain tumor cell line U87. The viability of cells was determined using the MTS assay as previously described. Briefly stated, the cells were plated into 96 well plates at $0.5-2 \times 10^4$ per well, 24 h prior to drug treatment. Subsequently, the cells were treated with 0.01, 0.5, or 0.1 µM epirubicin with and without 1 μM temozolomide, or 0.1, 1, or 10 μM C-dot conjugates: C-dot-epi, C-dot-temo, C-dot-epi + temo, or 0.01, 0.05, or 0.1 µM C-dot-transferrin conjugates: C-dots-trans-epi (C-ET), C-dots-trans-temo (C-TT) and C-dots-trans-dual (both epirubicin and temozolomide) drugs (C-DT). After 72 h incubation, viability was examined using the CellTiter 96® Aqueous One Solution Cell Proliferation Assay (Promega) based on the manufacturer's instructions. The absorbance was measured at 490 nm using a BioTek Synergy HT Plate reader. Data are presented as the average of 3 separate experiments in which the viability was calculated as the percentage of non-treated cells. +Standard error of the mean (SEM) was calculated. Significance was determined using Student's t-test. The consistency of the data was confirmed using different batches of C-dot conjugates.

Results and discussion

The purpose of this study is to analyze the efficacy of the dual drugs with the targeted ligand on the same nano-carrier Paper Nanoscale

(C-dots) (triple system, C-DT) compared to the same drugs conjugated separately on C-dots (dual systems, C-TT and C-ET). Also, drugs have been loaded into C-dots with and without transferrin to prove the efficiency of the samples with transferrin. The samples without transferrin consist of C-dots-epi + temo, C-dots-epi, and C-dots-temo, while C-dots-trans-epi + temo (C-DT), C-dots-trans-epi (C-ET), and C-dots-trans-temo (C-TT) are the samples conjugated with transferrin (Fig. 2). Prior to the conjugation, carbon dots were synthesized via the top-down, acid oxidation method using carbon nano powder as the precursor which was previously reported by Li et al.²⁹ In the process of conjugation, carboxylic groups on C-dots were first activated by EDC and NHS and then the covalent conjugations were performed with transferrin and drugs.30,33 The conjugated samples were first dialyzed using the 3500 MWCO dialysis bag for 4 days to remove non-conjugated drugs and other small molecules. DI water was replaced every 4-10 h. Finally, the pre-dialyzed C-dots-transferrin conjugate samples were further purified by SEC to remove unbound transferrin molecules. The conjugated samples were characterized by UV-Vis, fluorescence, FTIR and MALDI-TOF spectroscopy and TEM and AFM imaging. The in vitro studies were performed with the pediatric brain tumor cell lines SIGBM2, CHLA200, and CHLA266 and the adult brain tumor cell line U87.

4.1. Characterization of C-dots-epirubicin and the activation process of temozolomide

From the UV-vis spectra (Fig. 3), the presence of epirubicin in triple conjugated C-DT can be confirmed and the activation process of temozolomide can be detected. The epirubicin (red) spectrum displayed a characteristic absorption peak at 487 nm. An absorption peak at the same wavelength (487 nm) can be seen in the triple conjugated C-DT (blue) spectrum, indicating the existence of epirubicin in C-DT.

The temozolomide (green) spectrum displayed a significant absorption peak at 330 nm, which clearly disappeared in the triple conjugated C-DT spectrum (blue). This can be explained

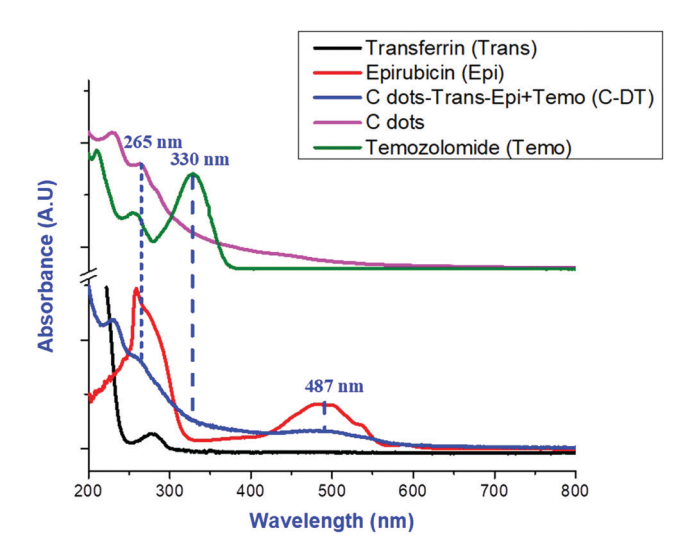


Fig. 3 UV-vis spectra comparison of free epirubicin (epi), C-dots, temozolomide (temo), and transferrin (trans) and the triple conjugation of C-dots-trans-epi-temo (C-DT). The samples (20 μ g mL $^{-1}$) were tested in a 1 cm optical quartz cell.

by the analysis of the electronic features of temozolomide and its metabolites by UV-vis absorption spectroscopy, which has been done by Khalilian $et~al.^{38}$ During the activation process of temozolomide, the tetrazinone ring becomes distorted with the addition of water to the carbonyl moiety and then tautomerization occurs with the elimination of CO_2 . The resulting methyltriazenylimidazole-4-carboxamide (MTIC) further converts to aminoimidazole-4-carboxamide (AIC) (Fig. S1†). Khalilian et~al. have further studied the variation of the absorption $\lambda_{\rm max}$ of temozolomide and its metabolites MTIC and AIC in PBS medium. The peak at 330 nm of temozolomide (green) is due to the π - π * transition of N=N, which disappeared in the AIC structure due to the breakage of the tetrazinone ring (Fig. S1†). The absorption peak of AIC at 265 nm is

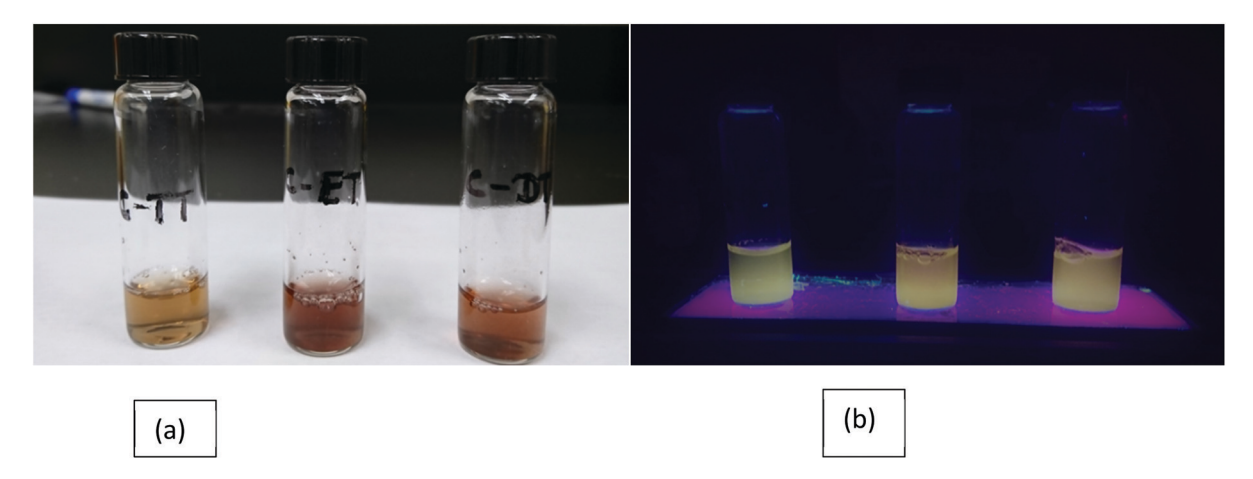


Fig. 2 Images of transferrin conjugated samples: C-dots-trans-temo (C-TT), C-dots-trans-epi (C-ET), and C-dots-trans-temo + epi (C-DT) (from left to right, respectively): (a) under white light and (b) UV light (365 nm).

overwhelmed (in the triple conjugated C-DT spectrum (blue)) by the absorption peak of C-dots (pink). The characteristic absorption peak of C-dots at 265 nm is due to the transition of $n-\pi^*$ of C=O (Fig. 3). Therefore the disappearance of the peak at 330 nm in the C-DT (blue) spectrum can possibly be due to the structural change of temozolomide to AIC.

4.2. Characterization of C-dots-transferrin-epirubicintemozolomide (C-DT)

The best analysis methods to describe the conjugation of transferrin on C-dots are fluorescence and MALDI-TOF spectroscopy.

Transferrin, epirubicin and C-dots have different fluorescence emission spectra (Fig. S1-S3 in the ESI†), which are clearly distinguished in the spectrum of the triple conjugated system (C-DT) (Fig. 4). The fluorescence emission spectrum of free transferrin has a peak at 346 nm when excited at 280 nm (Fig. S2†) while an emission peak is observed at 343 nm in the triple conjugated C-DT emission spectrum when excited at 280 nm (Fig. 4). The minor 3 nm blue shift of transferrin in the C-DT spectrum is only due to the attachment of transferrin on C-dots.

The fluorescence spectrum of epirubicin (Fig. S3†) displayed two emission peaks at 557 and 592 nm when excited at 480 nm. Even in the triple conjugated system (C-DT) (Fig. 4), two emission peaks were observed at 551 and 590 nm when excited at 480 nm. The fluorescence spectroscopy further confirms the presence of epirubicin in the conjugated system with a narrow blue shift. Furthermore, when C-DT was excited at different wavelengths (280-460 nm), a wavelength dependency was observed (Fig. 4), which is a characteristic feature of C-dots only (Fig. S4†). Therefore, fluorescence spectroscopy is

an analytical method that has verified the conjugation of both transferrin and epirubicin on C-dots.

Further characterization was performed by Fourier transform infrared spectroscopy (FTIR-ATR) to observe the structural changes in temozolomide and its conjugation on C-dots.

4.3. Characterization of the conjugation of C-dotstemozolomide

The conjugation of temozolomide on C-dots can be characterized by FTIR-ATR spectroscopy. In Fig. 5(a), a weak N-H stretching peak was observed in the C-dots-temo (blue) spectrum at 3380 cm⁻¹. It was sharply overlapped with the N-H stretching peak in the spectrum of free temozolomide (black) (shown as the dark green dotted line), which confirmed the presence of temozolomide on C-dots (Fig. 5(a)). Also, a new peak was observed at 1338 cm⁻¹ in the C-dots-temo (blue) spectrum in Fig. 5(a), which belongs to the C-N stretching peptide bond. This appeared after the covalent conjugation of temozolomide -NH₂ with the -COOH of C-dots. ^{39,40} Therefore, the formation of the C-N peptide bond further confirmed the conjugation of temozolomide on C-dots.

The structural change of temozolomide can be further detected by FTIR-ATR spectroscopy. In the spectrum of C-dotstemo (blue) shown in Fig. 5(a), the N=N vibration peak at 1595 cm⁻¹ barely appeared, compared with the black spectrum of temozolomide (the dark red dotted line). 40 This is possibly due to the structural change of temozolomide to AIC (Fig. S1†), because the N=N bond disappeared in AIC due to the breakage of the tetrazinone ring of temozolomide. Therefore, the FTIR-ATR spectroscopy also barely confirms the presence of AIC instead of temozolomide in the conjugation.

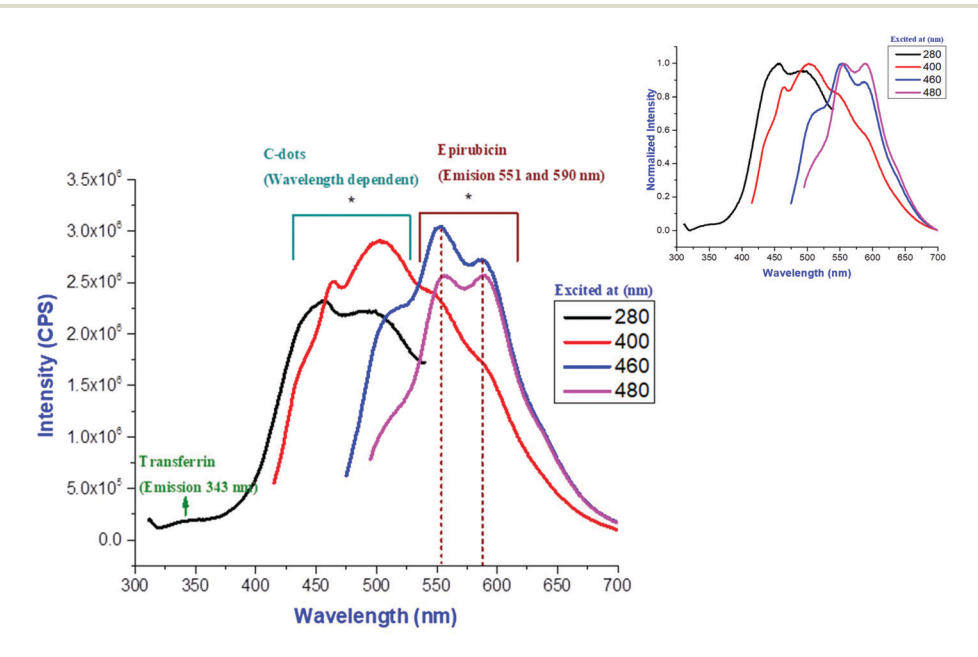


Fig. 4 The fluorescence emission spectra of the triple system C-dots-trans-epi-temo (C-DT) at different excitation wavelengths. The sample was tested with a slit width of 5 nm for both excitation and emission. Inset: Normalized fluorescence emission spectra. The C-DT sample was tested at 10 μ g mL⁻¹ concentration in a 1 cm (optical path length) quartz cell.

Paper Nanoscale

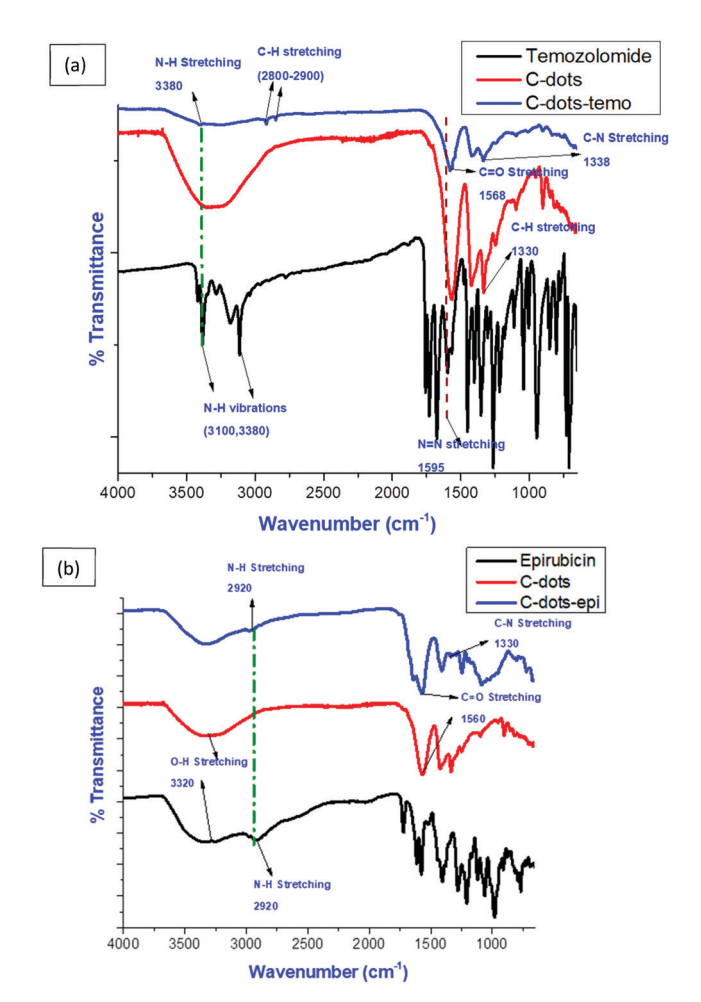


Fig. 5 FTIR-ATR spectra comparison of (a) C-dots, temozolomide and C-dots-temozolomide (C-dots-temo) conjugation and (b) C-dots, epirubicin and C-dots-epirubicin (C-dots-epi) conjugation.

Fig. 5(b) further confirms the conjugation of C-dots and epirubicin. In the spectrum of C-dots-epi (blue) (Fig. 5(b)), the N-H stretching peak at 2920 cm⁻¹ was overlapped with the N-H stretching peak of free epirubicin (black) and the new stretching peak for the C-N bond appeared at 1330 cm⁻¹. This further confirmed the conjugation of epirubicin on C-dots.

The presence of each compound in C-DT was further confirmed by FTIR-ATR spectroscopy as shown in Fig. S7.† The peaks at 2920 and 2840 cm $^{-1}$ confirmed the existence of epirubicin and transferrin in C-DT, the C=O stretching peak at 1567 cm $^{-1}$ verified the presence of temozolomide in C-DT and finally the formation of a new C-N stretching peak at 1330 cm $^{-1}$ further confirmed the formation of a peptide bond.

4.4. Characterization of the conjugates by particle size

As shown in Fig. 6, the AFM and TEM images further revealed the conjugation of temozolomide, epirubicin, and transferrin on C-dots upon the particle size increment. The average particle sizes of AFM and TEM for C-dots (before the conjugation) were 1.5 and 1.7 nm, respectively, while the average particle sizes of TEM and AFM for triple conjugated C-dots (after the conju-

gation) were 2.6 and 3.5 nm, respectively. The size increment of the conjugated sample further supported the successful conjugation of transferrin, epirubicin and temozolomide on C-dots.

4.5. Characterization of the conjugates by mass

In addition, conjugated samples were characterized by MALDI-TOF mass spectroscopy. According to Fig. 7, all the conjugated samples were over $80\,000\,\mathrm{g}\,\mathrm{mol}^{-1}$ (higher than the free transferrin m/z ratio (Fig. S5†)), which confirmed the successful conjugation of transferrin on C-dots. The molecular weight of the C-dot is only around $850\,\mathrm{g}\,\mathrm{mol}^{-1}$ (Fig. S6†). Furthermore, compared to the mass of C-dots-transferrin (C-dots-trans), the mass of drug conjugated samples on C-dots-trans (C-DT, C-TT and C-ET) is higher. This revealed the successful conjugation of drugs on C-dots-trans.

Moreover, the triple system (C-DT) displayed a lower mass than the conjugates of each individual drug and transferrin on C-dots (dual systems) (C-TT and C-ET). This could possibly be due to the higher steric hindrance in the reaction mixture of the triple system than in the dual systems. In any case, MALDI-mass spectroscopy suggested that the triple system (C-DT) possibly has a lower number of drug molecules than either dual system (C-TT and C-ET). Furthermore, epirubicin calibration curve analysis indicated that C-DT has a lower concentration of loaded epirubicin than all other samples (Fig. S8 and Table S1†). Therefore, *in vitro* cell studies were performed to analyze the efficacy of the triple system (C-DT).

5. *In vitro* studies with glioblastoma brain tumor cell lines

The *in vitro* efficacy of triple conjugated C-DT was tested with pediatric and adult brain tumor cells: SJGBM2, CHLA200 (both being pediatric glioblastoma), U87 (adult glioblastoma) and CHLA 266 (a typical teratoid/rhabdoid tumor). The efficacy of the triple system (C-DT) was compared to that of a combination of free drugs (temozolomide and epirubicin) and C-dots-drug conjugates with and without transferrin.

5.1. Efficacy of the mixture of free drugs temozolomide and epirubicin

The combination of an anthracycline drug with a DNA alkylating agent drug has been shown to be effective for cancer patients in both *in vitro* and *in vivo* models. In order to determine the drug efficacy of the combination of temozolomide and epirubicin in brain tumor cell lines, cells were treated with increasing concentrations of epirubicin with and without 1 μ M temozolomide.

Temozolomide induced only a small decrease in the cell viability of pediatric cell lines: SJGBM2, CHLA200 and CHLA266 (Fig. 8A–D), while epirubicin induced a dose-dependent decrease in the viability of all cell lines. Mixtures of epirubicin and temozolomide further reduced viability in all cell lines and at some concentrations, the effect was more than additive, suggesting a possible synergistic effect. The lowest

0.75

1.25 1.5 1.75

Nanoscale

-2.5 -2.25 -2 -1.75 -1.5 -1.25-0.75-0.5 -0.25 um (a) (b) 1.5 o 0.25 0.5

Fig. 6 (a) AFM and (b) TEM topology images of free C-dots; (C) AFM and (d) TEM topology images of C-dots-transferrin-epirubicin-temozolomide (triple system) (C-DT). The scale bars in both the TEM images represent 10 nm. The carbon dot solutions were sonicated for 15 min before the analysis.

cell viabilities were shown by the mixture of epirubicin and temozolomide at the highest concentration of epirubicin. The combined treatment of 0.1 μM epirubicin and 1 μM temozolomide reduced the viability to approximately 15–20% of nontreated controls except for the U87 cell line, which appeared to be more resistant and reduced the viability only to 45%. However, the combined treatment of epirubicin and temozolomide was more effective than epirubicin alone in each cell line, confirming that the epirubicin and temozolomide combination is a better choice for inhibiting these brain tumor cell lines. But the current concern is that we still need high concentrations of drugs to reduce the cancer cell viability, potentially harming

(C)

non-cancerous cells. Next, we examined whether C-dots would be a suitable nanocarrier and whether the chemotherapies conjugated with C-dots would still be effective.

5.2. Efficacy of C-dots-drug conjugates (non-transferrin)

(d)

C-dots-drug conjugated samples of C-dots-epi, C-dots-temo and C-dots-epi + temo were tested at increasing concentrations (0.1–10 μ M) on brain tumor cell lines. As shown in Fig. 9, C-dots-temo was relatively ineffective at reducing the cell viability in all types of tumor cell lines. In contrast, all concentrations of C-dots-epi and C-dots-epi + temo significantly reduced viability in all cell lines (Fig. 9A–D). Among all three

Paper Nanoscale

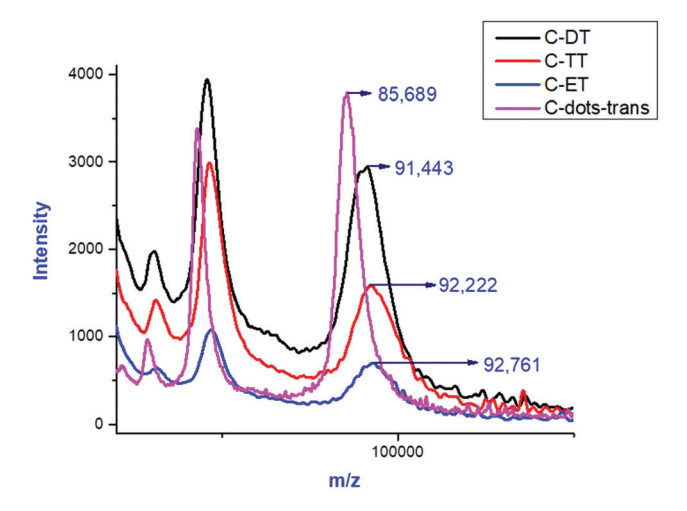


Fig. 7 MALDI-TOF spectra of transferrin conjugated samples of C-dots-transferrin (C-dots-trans), C-dots-transferrin-epirubicin-temo-zolomide (C-DT) (triple system), C-dots-transferrin-temozolomide (C-TT), and C-dots-transferrin-epirubicin (C-ET). The consistency of the data has been confirmed by batch-to-batch analysis.

conjugates, C-dots-epi + temo induced a substantial loss of cell viability, especially at the concentrations of 1 and 10 µM. The viability of C-dots-epi at 10 μM was 17-30% in all the cell lines (average compared to non-treated controls), while the viability of C-dot-epi + temo was significantly reduced to 7-21%. This reveals the higher efficiency of dual drug conjugation on the same C-dot compared to single drug conjugation. Anyhow, to obtain a significant reduction of cell viability, the required concentrations of C-dots-epi + temo are much higher than those of the free drugs. This might be due to most of the C-dots-drug conjugates having been pumped off from the cell membrane drug efflux pumps. The most popular p-glycoprotein (p-gp) drug efflux pump inhibitors are verapamil, Cyclosporin A, transflupenthxol, second generation inhibitors of D-isomer of dexverapamil, and etc. 43 Neither epirubicin nor temozolomide blocks the drug efflux pumps. As described in the introduction, these drugs are only DNA alkylating/methylating agents and DNA synthesis inhibitors. 35-37 This may be due to the lack of a cell targeting ligand and underscores the necessity to develop cancer cell targeted drug delivery systems. Using an appropriate

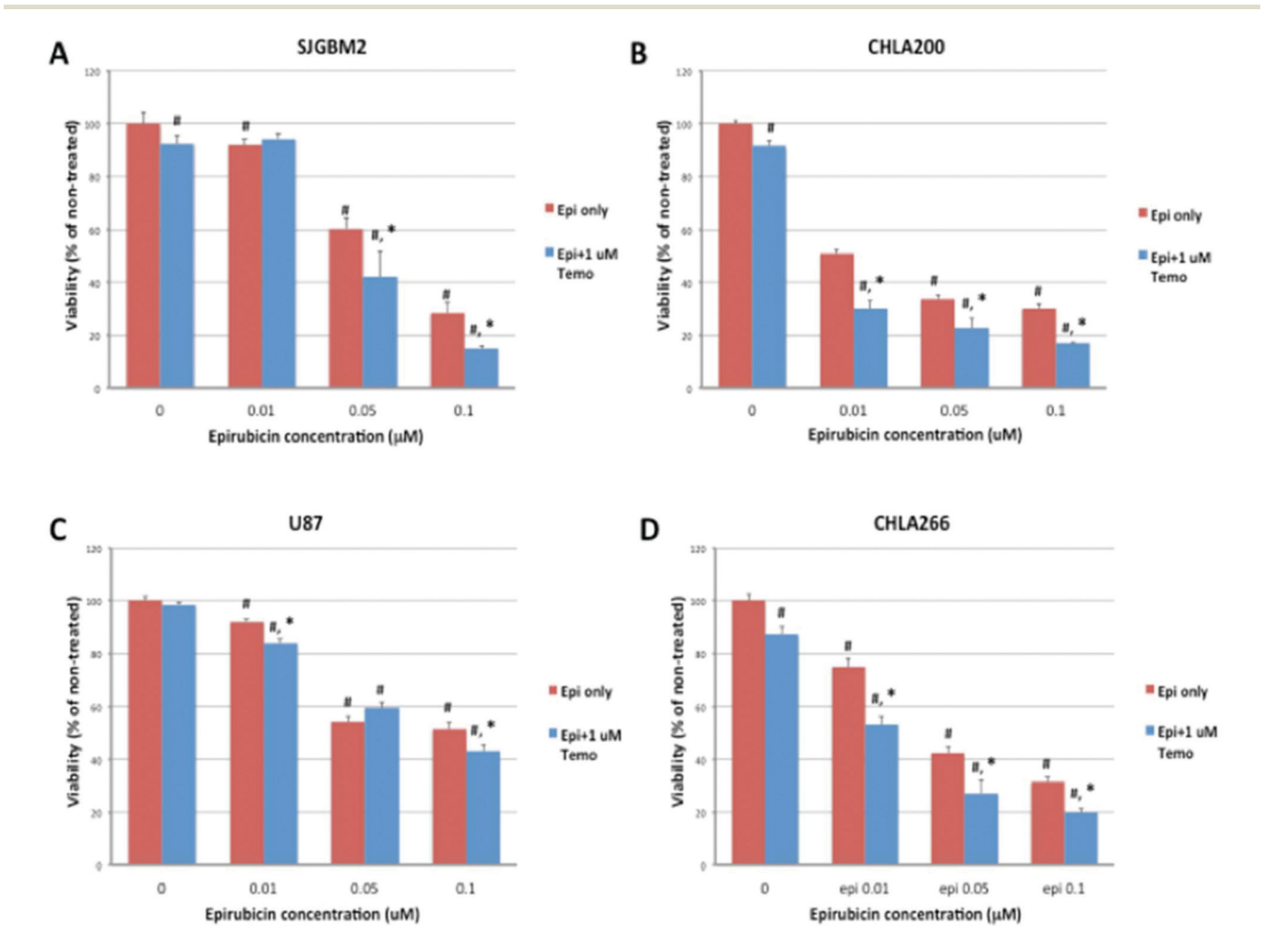


Fig. 8 Cell viability of the brain tumor cell lines (A) SJGBM2, (B) CHLA200, (C) U87 and (D) CHLA266 exposed to free temozolomide, free epirubicin or a mixture of temozolomide and epirubicin treatment. Data are presented as a percentage of non-treated control cells \pm SEM. #p < 0.05 compared to the control; *p < 0.05 comparing the combined drug treatment to free epirubicin.

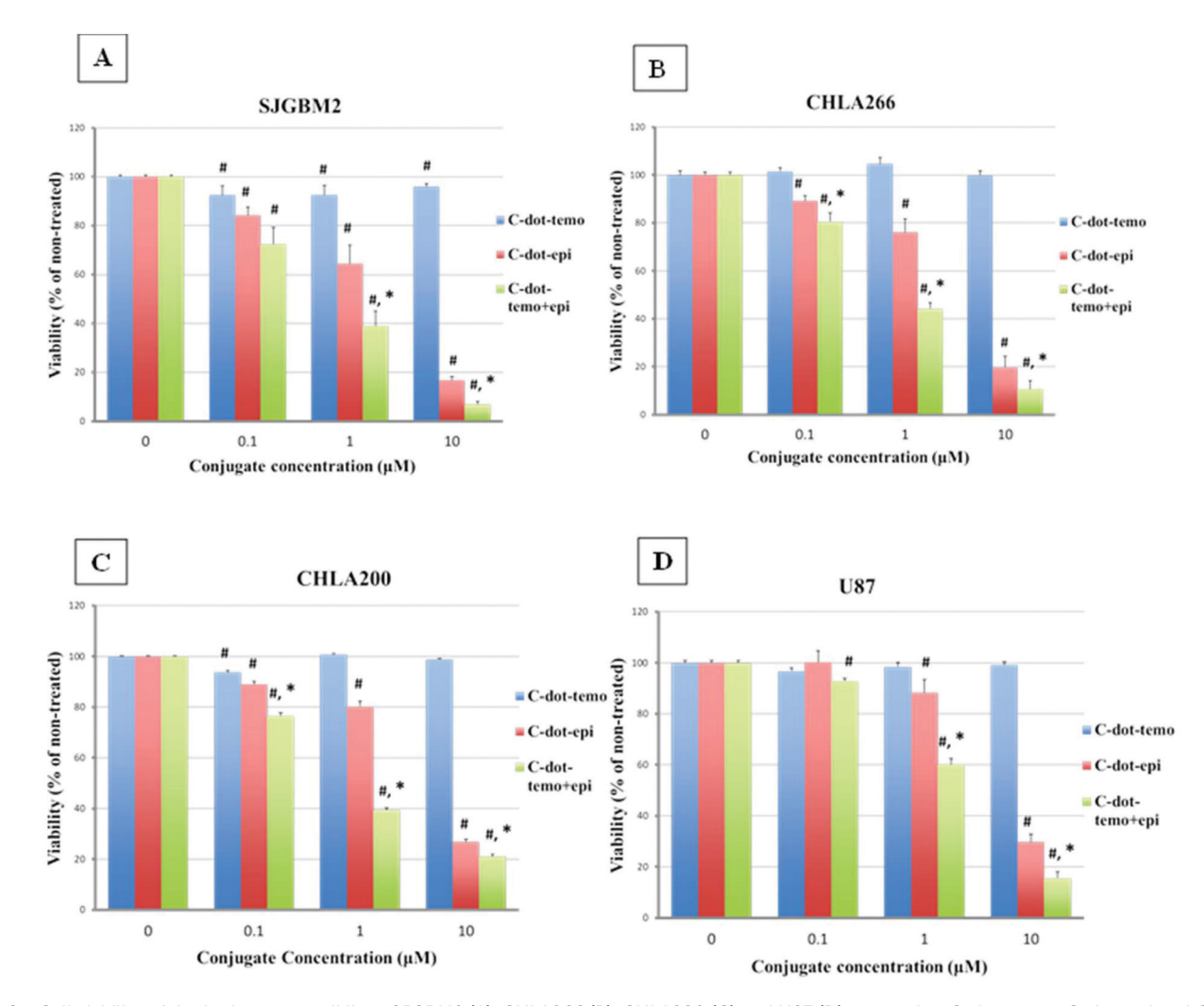


Fig. 9 Cell viability of the brain tumor cell lines SJGBM2 (A), CHLA266 (B), CHLA200 (C) and U87 (D) exposed to C-dot-temo, C-dot-epi and C-dotepi + temo. Data are presented as percentage of non-treated control cells + SEM. #p < 0.05 compared to the control, *p < 0.05 comparing C-dotepi to C-dot-epi + temo.

targeted system will result in greater cellular uptake and increase the anticancer activity of the C-dots-drug conjugates. Since most of the tumor cell lines have an overexpression of transferrin receptors on the membrane, transferrin will enhance cell penetration since it enters the cell via receptor mediated endocytosis. Therefore, the next set of samples tested with brain tumor cell lines were transferrin conjugated C-dots-drugs.

5.3. Efficacy of C-dots-drugs-transferrin conjugates (with transferrin)

Three transferrin conjugated samples were analyzed on the same cell lines as above. Transferrin receptor expression in these cell lines was confirmed by immunocytochemistry (Fig. S9†). The triple conjugated system C-dots-transferrin-temozolomide-epirubicin (C-DT) and the dual conjugates (but a single drug in each conjugate) C-dots-transferrin-temozolomide (C-TT) and C-dotstransferrin-epirubicin (C-ET) were tested at increasing concentrations of 0.01-0.1 µM. After the conjugation of transferrin with C-dots-drugs, the cell viability was drastically reduced even at a

lower concentration compared to the C-dots-drug conjugates without transferrin (Table 1). Also, among the three transferrin conjugated samples, the triple system (C-DT) displayed lower cell viability than either dual system (C-TT and C-ET).

One of the dual systems, C-dot-transferrin-temozolomide (C-TT), showed only a minimal effect on cell viability. C-TT displayed the lowest cell viability of 75% only at 0.1 µM in U87 (Fig. 10D). But the epirubicin conjugated system C-ET showed cell viabilities of around 20% in the most sensitive cell line SJGBM2 at 0.05 µM and 10% at a concentration of 0.1 µM in CHLA266 (Fig. 10A).

On the other hand, the triple system C-DT showed the lowest cell viability of 14% even at the lowest concentration of 0.01 µM in the most sensitive cell line SJGBM2 and 18% at 0.05 µM in CHLA266. Even though C-DT and C-ET both displayed the lowest cell viability in CHLA200 and U87 at 0.1 µM, C-ET only reduced the cell viability to 30 and 50%, while C-DT decreased the viability to 15 and 20% in CHLA200 and U87, respectively (Fig. 10).

Table 1 Average cell viability (all four cell lines) comparison of the non-transferrin and transferrin conjugated samples at their lowest concentrations. All the abbreviations are as follows: C-dots-epirubicin (C-dots-epi), C-dots-temozolomide (C-dots-temo), C-dots-epirubicin + temozolomide (C-dots-epi + temo), C-dots-transferrin-temozolomide (C-TT), C-dots-transferrin-epirubicin (C-dots-epi), and C-dots-transferrin-epirubicin-temozolomide (C-DT)

Concentration (µM)	Average cell viability (%) of the cell lines SJGBM2, CHLA266, CHLA200, and U87					
	Without transferrin			With transferrin		
	C-dots-temo	C-dots-epi	C-dots-temo + epi	C-TT	C-ET	C-DT
10.0	98.20	23.20	13.50	_	_	
1.0	99.12	77.27	45.6	_	_	_
0.1	96.12	90.65	80.5	86.60	24.30	11.60
0.05	_	_	_	91.20	36.20	27.40
0.01	_	_	_	95.90	61.15	43.55

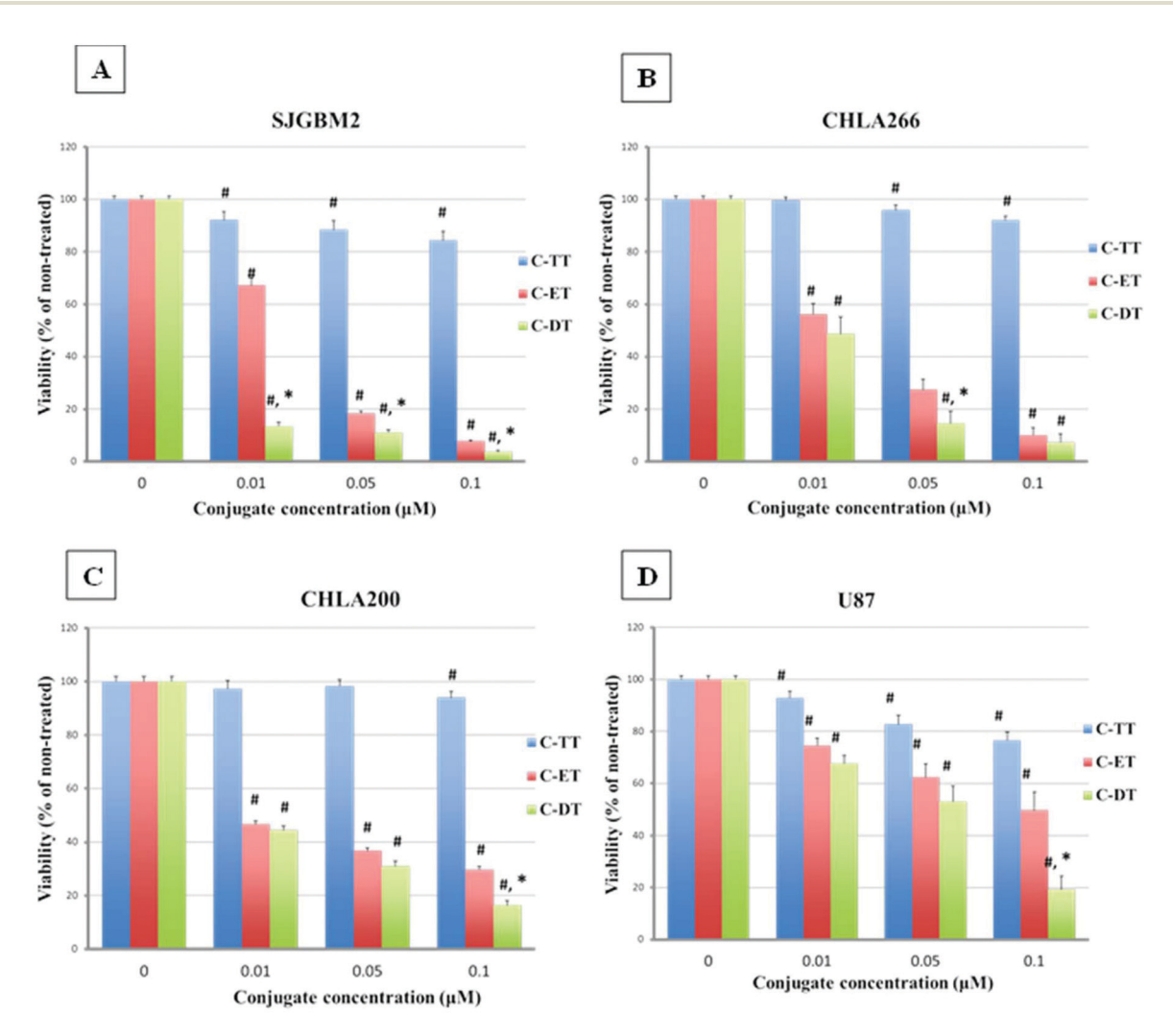


Fig. 10 Cell viability of the brain tumor cell lines SJGBM2 (A), CHLA266 (B), CHLA200 (C) and U87 (D) exposed to C-dot-temo-trans (C-TT), C-dot-epi-trans (C-ET) and C-dot-epi + temo-trans (C-DT). Data are presented as a percentage of non-treated control cells \pm SEM. #p < 0.05 compared to the control, *p < 0.05 comparing C-ET to C-ET.

Overall, the addition of transferrin increased the cytotoxicity even at a lower concentration than that without transferrin (Table 1). Similarly, we observed the nuclear epirubicin fluorescence of transferrin conjugated C-dots at much lower concentrations compared to the non-transferrin conjugated C-dots (Fig. S10 and S11†), indicating that the addition of transferrin increases cellular uptake of the C-dot-drug conjugates and therefore cell death. Furthermore, among transferrin conjugated samples, the triple conjugated system (C-DT) increased the cytotoxicity at a lower concentration than the other two conjugates.

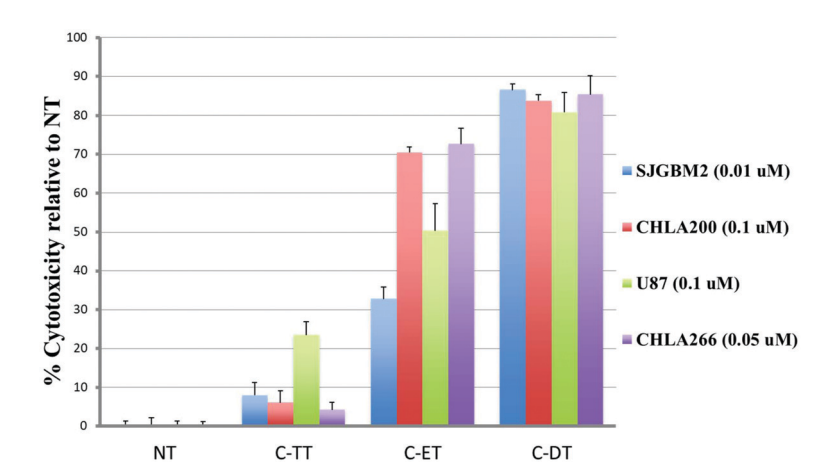


Fig. 11 Cytotoxicity profiles of the three transferrin conjugated samples C-TT, C-ET and C-DT on each cell line compared to the non-treated sample (NT). The concentration in each cell line represents the lowest effective concentration of the triple conjugated C-DT that causes the maximum cytotoxicity and the synergistic effect.

C-dot conjugate

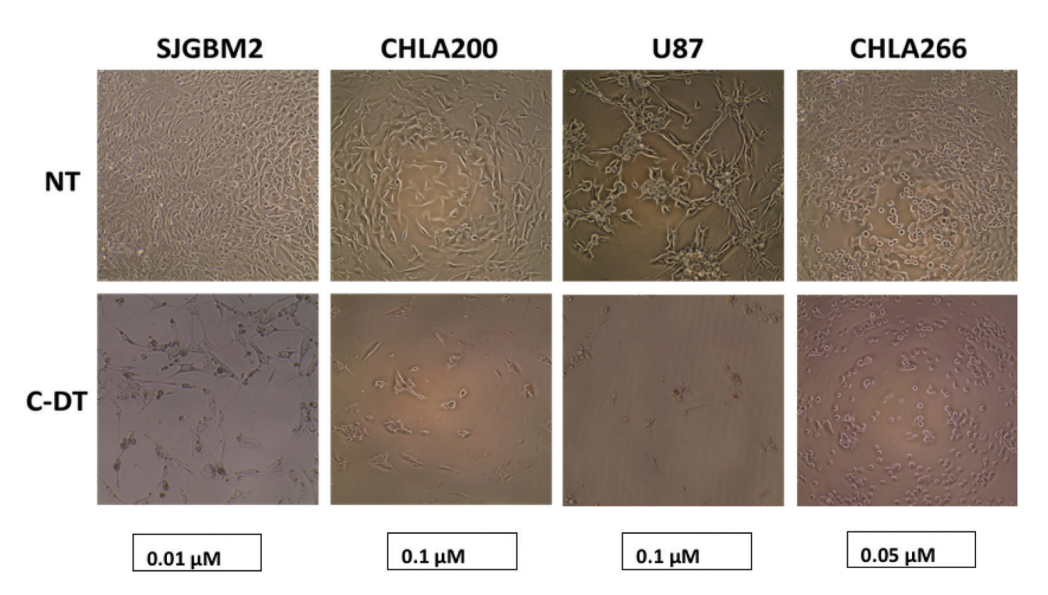


Fig. 12 Morphology images of each cell line (SJGBM2, CHLA200, U87, or CHLA266) of non-treated (NT) and C-DT treated samples at the concentrations of 0.01, 0.1, 0.1 and 0.05 μ M, respectively.

5.4. Synergistic effect of the triple system C-DT

As discussed above in the characterization section, MALDImass spectroscopic data revealed that the triple conjugated system (C-DT) has a lower number of drug molecules (even though both drugs were conjugated together on C-dots) than either dual system (with only a single drug conjugated on C-dots) (C-TT and C-ET). Moreover, Fig. 11 further shows that the triple conjugate (C-DT) not only increased the cytotoxicity, even with a lower number of drug molecules, but the two-drug combination displayed a synergistic effect. For instance, 0.01 µM C-DT in SJGBM2 induced 86% cell death whereas C-TT induced 8% and C-ET induced 33% cell death (Fig. 11). The sum of C-TT and C-ET is only 41%, but C-DT itself increased the cytotoxicity to 86%, which further confirmed the

efficiency of the triple conjugated C-DT. The representative morphology images of each cell line of non-treated and C-DT treated samples are shown in Fig. 12. The cell density reduction was clearly seen after treating each cell line with triple conjugated C-DT. The images of each cell line were taken at the lowest effective concentration of C-DT, which showed the highest cell density reduction and the highest synergistic effect.

Conclusion 6.

In this study we have successfully developed a triple conjugated (including two drugs) targeted nano drug delivery system

Paper Nanoscale

that displays a synergistic effect for the brain tumor cell lines. Transferrin, epirubicin, and temozolomide were conjugated on the same C-dot. The successful conjugation of each ligand was confirmed by UV-vis, fluorescence, FTIR and MALDI-TOF spectroscopy and TEM and AFM imaging. MALDI analysis further revealed that C-DT might have a lower number of conjugated drugs than C-TT and C-ET. In vitro studies showed that transferrin conjugated samples showed drastically reduced cell viability compared to non-transferrin conjugates. Among the three transferrin conjugated samples, the triple system (C-DT) is more cytotoxic to glioblastoma brain tumor cell lines than either dual system (C-TT and C-ET). Only a concentration of 0.01 µM was required by the triple system C-DT to reduce the cell viability to 14% in SJGBM2. Finally, we confirmed that the triple conjugated system (epirubicin, temozolomide and transferrin) on C-dots (C-DT) is a better therapeutic agent than the corresponding single drug delivery systems.

Conflicts of interest

There are no conflicts to declare.

Acknowledgements

We greatly appreciate the generous funding support given by NIH grant no. GR-009887 and NSF grant no. GR-011298. Also, we extend our deepest gratitude to the Mystic Force Foundation for providing us with the funding support for cell studies.

References

- 1 S. C. Curtin, A. M. Miniño and R. N. Anderson, Declines in Cancer Death Rates Among Children and Adolescents in the United States, 1999-2014, US Department of Health & Human Services, Centers for Disease Control and Prevention, National Center for Health Statistics, 2016.
- 2 D. Sturm, S. M. Pfister and D. T. Jones, J. Clin. Oncol., 2017, 35, 2370-2377.
- 3 M. Koshy, J. L. Villano, T. A. Dolecek, A. Howard, U. Mahmood, S. J. Chmura, R. R. Weichselbaum and B. J. McCarthy, J. Neuro-Oncol., 2012, 107, 207–212.
- 4 Q. Wu, Z. Yang, Y. Nie, Y. Shi and D. Fan, Cancer Lett., 2014, 347, 159-166.
- 5 Y. Yan, M. Björnmalm and F. Caruso, ACS Nano, 2013, 7, 9512-9517.
- 6 M. Y. Hanafi-Bojd, M. R. Jaafari, N. Ramezanian, M. Xue, M. Amin, N. Shahtahmassebi and B. Malaekeh-Nikouei, Eur. J. Pharm. Biopharm., 2015, 89, 248-258.
- 7 X. Wang, L. Yang and D. M. Shin, CA-Cancer J. Clin., 2008, 58, 97-110.
- 8 D. Peer, J. M. Karp, S. Hong, O. C. Farokhzad, R. Margalit and R. Langer, Nat. Nanotechnol., 2007, 2, 751.

- 9 J. Fang, H. Nakamura and H. Maeda, Adv. Drug Delivery Rev., 2011, 63, 136-151.
- 10 R. Cheng, F. Meng, C. Deng, H.-A. Klok and Z. Zhong, Biomaterials, 2013, 34, 3647-3657.
- 11 V. Torchilin, Adv. Drug Delivery Rev., 2011, 63, 131-135.
- 12 J. Gong, M. Chen, Y. Zheng, S. Wang and Y. Wang, J. Controlled Release, 2012, 159, 312-323.
- 13 J.-Z. Du, X.-J. Du, C.-Q. Mao and J. Wang, J. Am. Chem. Soc., 2011, 133, 17560-17563.
- 14 Y. Zhou, Z. Peng, E. S. Seven and R. M. Leblanc, J. Controlled Release, 2017, 290-303.
- 15 A.-C. Luissint, C. Artus, F. Glacial, K. Ganeshamoorthy and P.-O. Couraud, Fluids Barriers CNS, 2012, 9, 23.
- 16 D. J. Begley, Pharmacol. Ther., 2004, 104, 29-45.
- 17 I. Matai, A. Sachdev and P. Gopinath, ACS Appl. Mater. Interfaces, 2015, 7, 11423-11435.
- 18 J. Xie, S. Lee and X. Chen, Adv. Drug Delivery Rev., 2010, 62, 1064-1079.
- 19 P. Parhi, C. Mohanty and S. K. Sahoo, Drug Discovery Today, 2012, 17, 1044-1052.
- 20 J.-M. Shen, F.-Y. Gao, T. Yin, H.-X. Zhang, M. Ma, Y.-J. Yang and F. Yue, Pharmacol. Res., 2013, 70, 102-115.
- 21 B. Song, C. Wu and J. Chang, Acta Biomater., 2012, 8, 1901-
- 22 S. Aryal, C. M. J. Hu and L. Zhang, Small, 2010, 6, 1442-1448
- 23 V. P. Chauhan, T. Stylianopoulos, J. D. Martin, Z. Popović, O. Chen, W. S. Kamoun, M. G. Bawendi, D. Fukumura and R. K. Jain, Nat. Nanotechnol., 2012, 7, 383-388.
- 24 N. Hoshyar, S. Gray, H. Han and G. Bao, Nanomedicine, 2016, 11, 673-692.
- 25 G. L. Hornyak, H. F. Tibbals, J. Dutta and J. J. Moore, Introduction to nanoscience and nanotechnology, CRC press,
- 26 A. Zhao, Z. Chen, C. Zhao, N. Gao, J. Ren and X. Qu, Carbon, 2015, 85, 309-327.
- 27 I. P.-J. Lai, S. G. Harroun, S.-Y. Chen, B. Unnikrishnan, Y.-J. Li and C.-C. Huang, Sens. Actuators, B, 2016, 228, 465-470.
- 28 S. Li, Z. Peng and R. M. Leblanc, Anal. Chem., 2015, 87, 6455-6459.
- 29 S. Li, L. Wang, C. C. Chusuei, V. M. Suarez, P. L. Blackwelder, M. Micic, J. Orbulescu and R. M. Leblanc, Chem. Mater., 2015, 27, 1764-1771.
- 30 S. Li, D. Amat, Z. Peng, S. Vanni, S. Raskin, G. De Angulo, A. M. Othman, R. M. Graham and R. M. Leblanc, Nanoscale, 2016, 8, 16662-16669.
- 31 L. Wu, M. Luderer, X. Yang, C. Swain, H. Zhang, K. Nelson, A. J. Stacy, B. Shen, G. M. Lanza and D. Pan, Theranostics, 2013, 3, 677.
- 32 Y.-F. Wu, H.-C. Wu, C.-H. Kuan, C.-J. Lin, L.-W. Wang, C.-W. Chang and T.-W. Wang, Sci. Rep., 2016, 6, 21170.
- 33 Z. E. H. Miyanji, Y. Zhou, J. Pardo, S. D. Hettiarachchi, S. Li, P. L. Blackwelder, I. Skromne and R. M. Leblanc, Nanoscale, 2017, 9, 17533-17543.
- 34 Z. Qian, J. Ma, X. Shan, H. Feng, L. Shao and J. Chen, Chem. - Eur. J., 2014, 20, 2254-2263.

- 35 J. Pardo, Z. Peng and R. Leblanc, Molecules, 2018, 23, 378.
- 36 M. Tariq, M. A. Alam, A. T. Singh, A. K. Panda and S. Talegaonkar, Drug Delivery, 2016, 23, 2990-2997.
- 37 S. Kumari, S. M. Ahsan, J. M. Kumar, A. K. Kondapi and N. M. Rao, Sci. Rep., 2017, 7, 6602.
- 38 M. H. Khalilian, S. Mirzaei and A. A. Taherpour, J. Mol. Model., 2016, 22, 270.
- 39 M. Faizan, S. A. Bhat, M. J. Alam, Z. Afroz and S. Ahmad, J. Mol. Struct., 2017, 1148, 89-100.
- 40 M. Łaszcz, M. Kubiszewski, Ł. Jedynak, M. Kaczmarska, Ł. Kaczmarek, W. Łuniewski, K. Gabarski, A. Witkowska, K. Kuziak and M. Malińska, Molecules, 2013, 18, 15344-15356.
- 41 E. S. Villodre, F. C. Kipper, A. O. Silva, G. Lenz and P. L. da Costa Lopez, Mol. Neurobiol., 2018, 55, 4185-4194.
- 42 R. Zhang, R. Saito, I. Shibahara, S. Sugiyama, M. Kanamori, Y. Sonoda and T. Tominaga, J. Neuro-Oncol., 2016, 126, 235-242.
- 43 M. L. Amin, Drug Target Insights, 2013, 7, 27-34.